وزارة
التعليم العالي والبحث العلمي
جامعة ميسان
كلية التربية الاساسية

مجلة ميسان للدراسات الاكاديمية

مجلة ميسان للدراسات الأكاديمية

للعلوم الانسانية والاجتماعية والتطبيقية

Misan Journal For Academic Studies
Humanits, Social and applied Sciences

ISSN (Print) 1994-697X

(Online)-2706-722X

المجلد 24 العدد 56 كانون الاول

Dec 56 Issue 24 vol

Misan Journal

MISAN JOURNAL FOR ACADEMIC STUDIES
HUMANITS, SOCIAL AND APPLIED SCIENCES
VOLE 24 ISSUE 56 DEC,2025

MJAS

مجلة ميسان للدراسات الاكاديمية
العلوم الانسانية والاجتماعية والتطبيقية
كلية التربية الاساسية/ جامعة ميسان

المجلد 24 العدد 56 كانون الاول 2025

VOLE 24 SSUE56 DEC,2025

رقم الايداع في المكتبة الوطنية العراقية 1326 لسنة 2009

journal.m.academy@uomisan.edu.iq
https://www.misan-jas.com/index.php/ojs
https://iasj.rdd.edu.iq/journals/journal/view/298

MISAN JOURNAL FOR ACADEMIC STUDIES
HUMANITS, SOCIAL AND APPLIED SCIENCES
VOLE 24 ISSUE 56 DEC,2025

MJAS

ISSN (Print) 1994-697X
ISSN (Online) 2706-722X

DOI:
https://doi.org/10.54633/2333-024-056-007

Received:11/July/2025
Accepted:18/Sep/2025
Published online:30/Dec/2025

The Impacts of Nano Barium Titanate on The Radiopacity and Surface Roughness of 3D-Printed Acrylic Denture Base

Rand Naseer Kadhum*, Thekra Ismael Hamad
Department of Prosthodontic, Collage of Dentistry, University of Baghdad, Baghdad, Iraq
Email: rand.naseer2401m@codental.uobaghdad.edu.iq, thikra.ismail@codental.uobaghdad.edu.iq
ORCID: https://orcid.org/0009-0000-6087-2079.
* Corresponding Author Email: rand.naseer2401m@codental.uobaghdad.edu.iq

Abstract:

The creation of three dimensional (3D)-printed denture base was made possible by the advent of additive manufacturing technology. This research intends to test the effect of inclusion barium titanate nanoparticles ($BaTiO_3$NPs) at different weight percentages on the radiopacity and surface roughness of 3D-printable denture bases. Three groups were created: a control group, 0.5 wt.%, and 1 wt.% $BaTiO_3$NPs. Every sample was tested for surface roughness utilizing contact profilometer and atomic force microscope (AFM), and the radiopacity by measuring optical density using transmission densitometer. Adding $BaTiO_3$NPs to 3D-printable resin improved the radiopacity and decreased the surface roughness of the modified groups.

Keywords: Atomic force microscope, $BaTiO_3$NPs, Radiopacity, Surface roughness, 3D-printed denture base.

Introduction:

Complete dentures are usually given to patients with edentulous arches as a way to restore both appearance and functioning. Polymethylmethacrylate (PMMA) is the primary material used to make a full denture (Khalid et al., 2025). PMMA is a light weight, compatible, aesthetically beautiful substance that is simple to make and repair. Nevertheless, it is susceptible to fading and microbial adhesion and is impacted by exposure to various foods and drinks (Al-Rubaie & Al-Khafaji, 2024). It exhibits a decrease in polymerization and low mechanical and wear resistance (Gökay et al., 2021). It also has insufficient radiopacity (Abd Alrazaq & Khalaf, 2023). In order to get beyond the constrains of traditional methods and substances, denture fabrication has increasingly used inventive computer-aided design and computer-aided manufacturing (CAD-CAM) technology in the previous ten years (Alghazzawi, 2016). The application of three-dimensional (3D)

printing technologies to produce dental base resins has increased dramatically. Among its many advantages are accuracy and precision, which can lead to better tooth implantation and function. Additionally, little material waste and a quick manufacturing cycle result in lower manufacturing process costs (Tian et al., 2021).

Metals, fibers, ceramics, and oxides are examples of nanoparticles (NPs) that boost the mechanical and physical qualities of resin-based substances, leading to the creation of nanocomposites with improved qualities (Unkovskiy et al., 2021). The inherent qualities and kind of polymers employed, composites' processing method, size, concentration, and diffuseness of the NPs within the matrix of polymer, as well as the compatibility at the interface between the nanoparticles NPs and polymer matrix, all affect the overall performance of nanocomposites (Al-Rawi & Taha, 2015).

There have been a number of documented negative impacts, including decreased compatibility, formation of voids that lead to porosity, and the agglomeration of NPs that can result in stress-concentrated regions, which can then trigger the onset of fractures and crack propagation (Al-Sammraaie et al., 2024).

Barium titanate ($BaTiO_3$) is a polycrystalline ceramic substance with ferroelectricity and has a perovskite structure (ABO_3) (Ibrahim & Hamad, 2023). $BaTiO_3$ is widely used as a photocatalyst due to its cheap cost, chemical stability, and non-hazardous (Jiang et al., 2019).

The inclusion of barium titanate nanoparticles ($BaTiO_3$NP) to PMMA gave the denture base material increased flexural strength, increased surface hardness, and decrease roughness (Elshereksi et al., 2021), owing to the equally distributed and tightly compressed $BaTiO_3$NPs within the PMMA matrix.

To the maximum extent possible of the author's expertise, no previous study has examined how adding $BaTiO_3$NPs to 3D-printable resin influences surface roughness and radiopacity. According to the study's null hypothesis, adding 0.5% to 1% by weight of $BaTiO_3$NPs would not significantly affect the physical characteristics of the basic materials used for making 3D-printed dentures. However, according to the alternative hypothesis, physical qualities of the 3D-printable denture foundation will be improved when 0.5 and 1 weight percent are added.

Materials and Methods:

Following the guideline set forth by World Health Organization (WHO), the sample size of the study was established by analyzing power. The conclusions revealed a 5% marginal error, a 5% significance level, and an 80% study power.

Nanocomposite mixture preparation:

In order to create the samples for the nanocomposite dentures, a 3D-printed resin known as FREEPRINT® DENTURE was used in this study. Its components included dyes and additives, phosphine oxide as a photoinitiator, and a pink-transparent methacrylate base that was modified using 99.9% pure barium titanate nanopowder (Sky spring nanomaterial, Inc., USA) as the inorganic filler substance. The particle size analyzer (Nano Brook 90Plus, USA) showed that the particle’s average size was 71.4 nm. Pure resin was first mixed for 120 minutes in an LC-3D

mixer to guarantee resin homogeneity for creating the nanocomposite mixes (Alshaikh et al., 2022). $BaTiO_3$ nanoparticles were introduced to 3D-printed resin at percentages of 0.5 and 1wt.%, whereas one group (the control group) continued without adding any NPs. After adding carefully measured amounts of $BaTiO_3$NPs to different containers holding the base resin at the appropriate concentrations, the mixture was vigorously mixed using a mechanical mixer set to 2500 rpm for 5 minutes (Majeed et al., 2025; Zidan et al., 2019), the mixing process was performed in two stages to guarantee a uniform mixture (Altarazi et al., 2024). 60 specimens were printed: 30 for the radiopacity test (n=10) and 30 for surface roughness (n=10).

Specimens' preparation:

The specimens were made with 12 × 12 × 3 measurements in accordance with ISO 20795-1:2013 for surface roughness (ISO, 2013). For the radiopacity test, a disk-shaped specimen, which is 10 mm in diameter and 3 mm thick, was created and set on a wax plate of 3 mm thickness to encourage soft tissue's absorbing and dispersing media. For standardization, an aluminum (AL) step wedge was made by slicing a pure aluminum plate to the proper size and shape. It had ten steps, with the thickness of the aluminum growing by one millimeter at a time until the tenth step reached ten millimeters (ADA, 2000). The samples were designed utilizing CAD software, and standard tessellation language (STL) files, a popular file format for 3D printing, were exported. The planned models were then printed using an Asiga MAX UV 3D printer with a 0° orientation and a 50 µm layer thickness in order to achieve the required dimensions. The layers are then subjected to ultraviolet (UV) light with a wavelength of 405 nm, which initiates the polymerization process until a 3D-printed model is produced (Al-Dulaijan et al., 2023). Otoflash G171 was used for the post-curing process for 20 minutes in accordance with the company's guidelines. The procedure consisted of two cycles of 2000 flashes, each followed by a component turnaround, under an atmosphere of inert nitrogen gas. The samples were finally cleansed with 99.9% isopropyl alcohol, excess resin was scraped off. Then, in a wet condition, they were finished with a tungsten carbide bur at 1500 rpm and polished using emery paper. This process was carried out by a single operator to verify the comparable pressure of polishing instruments on specimens (Majeed et al., 2025). The samples are submerged in filtered water at 37°C for 48 hours prior to the test methodology (Al-Sammraaie et al., 2024). Sample's fabrication process demonstrated in Figure 1.

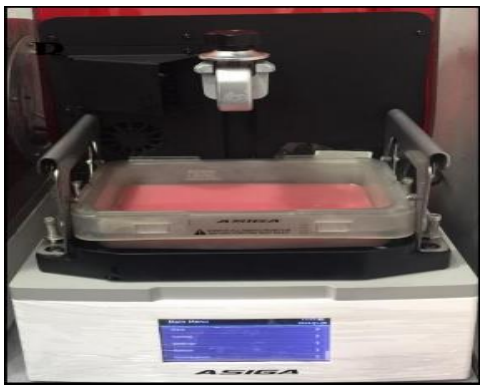

(a) (b)

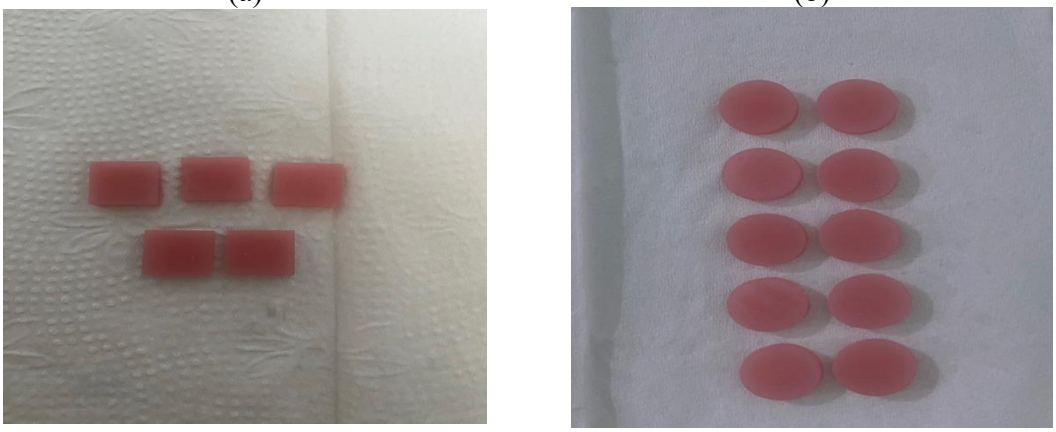

(c) (d)

Figure 1: Fabrication of 3D-printed specimens modified with $BaTiO_3$ (a) Resin loaded in the ASIGA 3D-printer (b) Light curing machine (c, d) Specimens after finishing and polishing.

Radiopacity test:

The specimen was positioned next to an AL step wedge to standardize the film's density. Using a chest x-ray machine (Philips, Germany), the exposure period was 0.38 seconds, the object-to-film distance was 1 meter, and the machine was run at 70 KV and 0.88 mAs, as shown in Figure 2. The variation in image density between all samples with varying concentrations of $BaTiO_3$NPs and the unmodified 3D-printed specimen and AL step wedge was measured using a light transmission densitometer (Pehamed Densonorm 21i, France), Figure 3. Each specimen underwent five measurements in various locations, and the average of these measurements was determined.

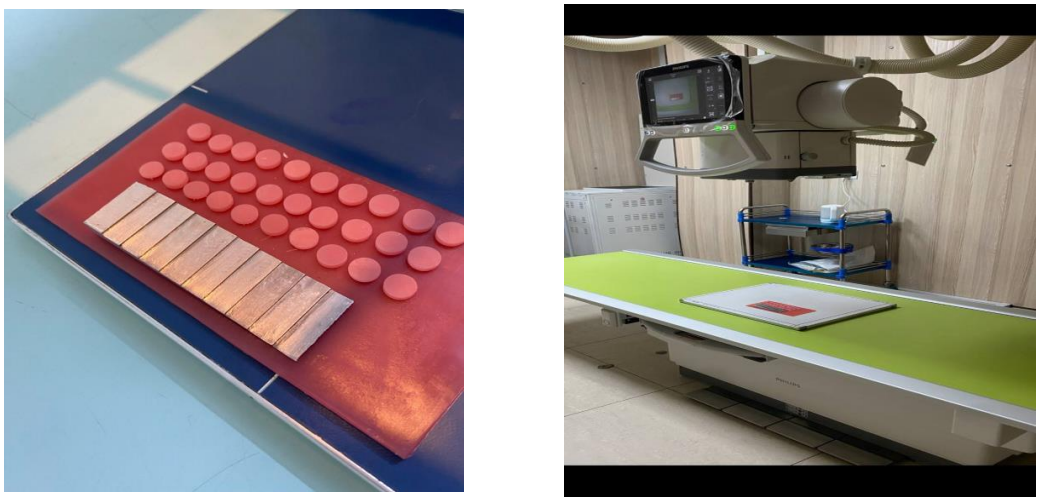

(a) (b)

Figure 2. (a) Specimens and AL step wedge on wax molds (b) Chest x-ray machine.

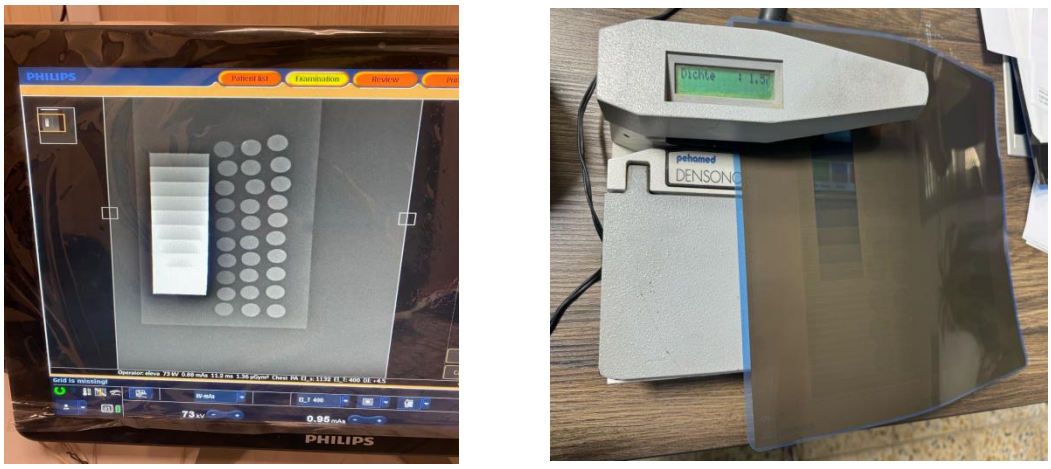

(a) (b)

Figure 3. (a) X-ray film for the specimens (b) Measuring the optical density of the x-ray films by densitometer.

Surface roughness

The surface roughness was measured in this study using a contact profilometer (JITA 810, China; Figure 4). The device has a sensitive diamond-tipped surface analyzer that allows it to follow the peculiarities of the specimen's topography. Because the instrument was set up so that its stylus only touched the surface of the specimen three times, three measurements were made for each specimen (Noori et al., 2023). When the stylus first made contact with one part of the specimen while it was on a firm and stable platform, an automatic digital scale readout emerged. Initial position readings guaranteed accuracy at first point contacts following surveying along a predetermined path that covered 11mm over authorized surfaces.

Figure 4. Contact profilometer for surface roughness measurement.

Fourier transmission infra-red spectrophotometer (FTIR):

By measuring the transmission of infrared rays at different frequencies, FTIR (Perkin Elmer, USA) is a potent analytical technique for identifying a compound's functional groups and determining if there is a chemical reaction between the nanoparticles and 3D-printable resin. One specimen from each of the following groups—one from the 0.5% $BaTiO_3$ group, one from the

1% $BaTiO_3$ group, and one from the control group—was brought to the FTIR equipment for the examination, The resolution range was 400–4000 cm^{-1}.

Atomic force microscope (AFM):

The surface topographies of 3D-printable samples are examined and compared, and their roughness is quantitatively assessed using an atomic force microscope (AFM model TT-2, USA). The specimen was set up on a magnetic disk-mounted sample holder. Using the tapping mode and a 15µm x 15µm scan area, the measurements were made.

Statistical analysis

The Statistical Package for Social Sciences (SPSS, Delaware/Chicago, version 29) was utilized to assess the research's findings. In order to compare each group's mean value, a one-way ANOVA was performed as part of the inferential analysis. Additionally, the data's normal distribution was determined utilizing Shapiro-Wilk test, and the homogeneity of variance was evaluated using Levene's test. Tukey's HSD post-hoc test (multiple comparisons) was working to ascertain whether the groups differed significantly from one another. A *p*-value of 0.05 or less was considered statistically significant (S), whereas a *p*-value of more than 0.05 ($p > 0.05$) was considered statistically non-significant (NS).

Results:

Radiopacity test:

Shapiro-Wilk test resulted that the data's distribution was normal, with a *p*-value more than 0.05, The outcomes indicated that the optical density decreased as the aluminum step wedge thickness increased, going from 1.44 at 1 mm AL thickness and 1.28 for 2mm AL thickness to 0.18 at 10 mm AL thickness. The optical density was higher in the control group (about 1.423), lower in the 0.5 wt.% group (mean value of 1.298), and lowest in the 1 wt.% group (mean value of 1.261), A statistically significant difference (S) (*p* value< 0.05) in optical density between the tested groups was shown using a one-way ANOVA (*p* value< 0.001), as demonstrated in Table 1 and Figure 5.

Table 1. Descriptive statistics, normality test, and ANOVA of radiopacity test.

Groups	**Mean**	**St. deviation**	***p*-value of Shapiro-Wilk test**	**Minimum**	**Maximum**	**F test by ANOVA**	***p*-value**
Control	1.423	0.035	0.805	1.37	1.48	27.852	<0.001
0.5 wt.%	1.298	0.062	0.070	1.20	1.36		
1 wt.%	1.261	0.058	0.094	1.21	1.35		

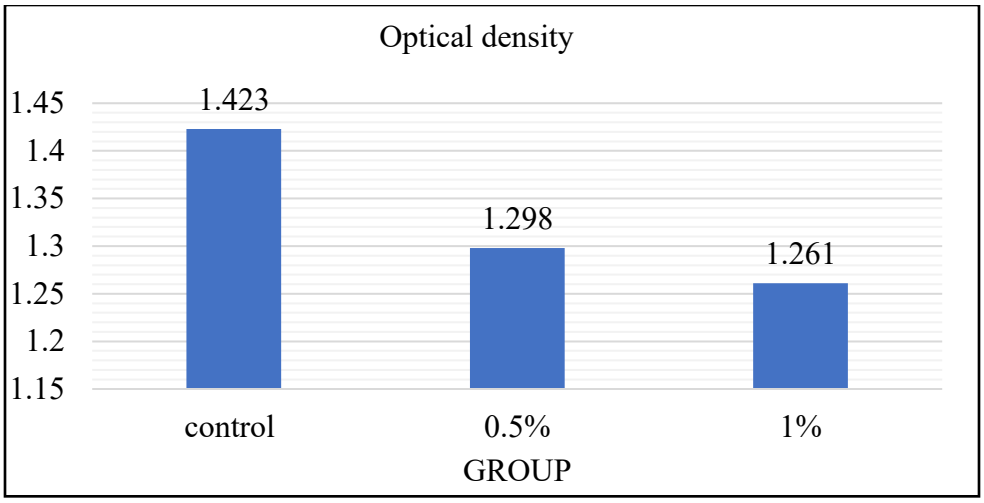

Figure 5. Bar chart of the optical density for the radiopacity test.

Having a *p*-value of 0.060 (*p*-value more than 0.05), Levene's homogeneity test was certain that there was no significant difference in the homogeneity of variances of the optical density measurements between the groups; consequently, the use of Tukey's HSD post hoc for multiple comparisons was made possible by this assumption. As presented in Table 2, Tukey's test revealed that optical density of the unmodified group and 0.5 wt.% and 1 wt.% groups differed significantly (*p*-value greater than 0.05); nevertheless, the difference between 0.5 wt.% and 1 wt.% modified groups was not significant (NS) (*p*-value more than 0.05).

Table 2. Post hoc multiple comparison of optical density for radiopacity test.

Groups	Mean difference	*P* Tukey
Control vs. 0.5 wt.%	0.12500	<0.001 S
Control vs. 1 wt.%	0.16200	<0.001 S
0.5 wt.% vs. 1 wt.%	0.03700	0.252 NS

Surface roughness:

Shapiro-Wilk test stated that the data was distributed normally with a *p*-value > 0.05. According to surface roughness tests, the unmodified group had the greatest average value (0.530µm), then 0.5wt.% group (0.355µm), and the 1wt.% group (0.292 µm), which had the lowest mean value. According to one-way ANOVA test, the surface roughness of the tested group differed statistically significantly (*p* <0.05) with a *p*-value of < 0.001; as seen in Table 3 and Figure 6.

Table 3. Descriptive statistics, normality test, and ANOVA for surface roughness test.

Groups	Mean (µm)	St. deviation	*P*-value of Shapiro-Wilk test	Minimum	Maximum	F-test by ANOVA	*P*-value
Control	0.530	0.084	0.758	0.42	0.68	30.010	<0.001
0.5 wt.%	0.355	0.070	0.420	0.23	0.44		
1 wt.%	0.292	0.056	0.831	0.20	0.38		

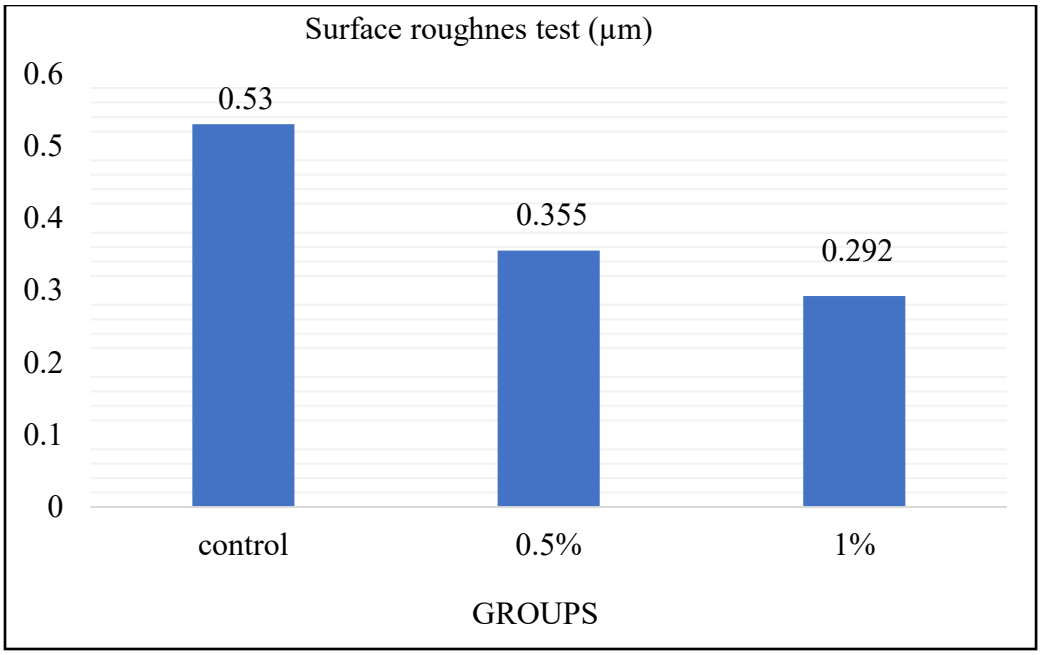

Figure 6. Bar chart surface roughness test.

Homogeneity of variance of surface roughness was not significant between the groups, according to Levene's test, which revealed a *p*-value of 0.378. Consequently, Tukey's post hoc test was worked for comparisons between the groups and showed that the surface roughness of 0.5 wt.% and 1 wt.% groups differed significantly (S) ($p < 0.05$) from that of the control (unmodified) group. While the difference between 0.5 wt.% and 1 wt.% groups was non-significant (NS) (p value > 0.05); Table 4 demonstrates the outcomes.

Table 4. Tukey's post hoc test of multiple comparison for surface roughness.

Groups	Mean differences	SE	*P*-value
Control vs. 0.5 wt.%	0.17500	0.3183	<0.001 S
Control vs. 1 wt.%	0.23800	0.3183	<0.001 S
0.5 wt.% vs. 1 wt.%	0.06300	0.3183	0.137 NS

FTIR:

FTIR findings showed that the modified specimens (containing 0.5 wt.% and 1 wt.% $BaTiO_3$NPs) and the unmodified specimens had identical spectra. The transmission peak alignment and pattern stayed constant; Figure 7 showed the FTIR spectra of the control, 0.5 wt.%, and 1 wt.% groups. This implies that $BaTiO_3$ NPs and the base substance for 3D-printed dentures have no chemical interaction, which is explained by particular functional groups that are present, as indicated in Table 5.

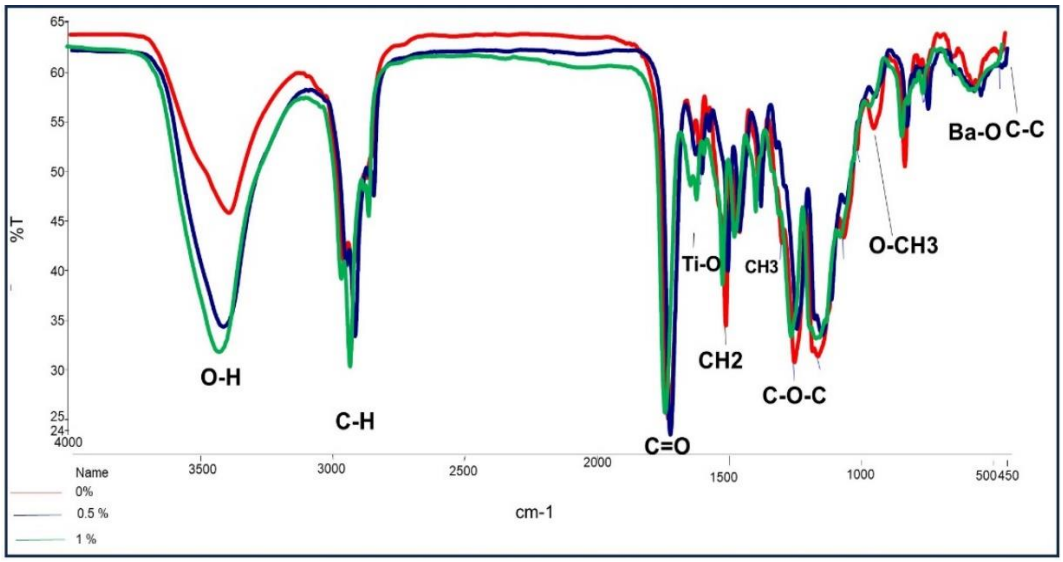

Figure 7. FTIR spectra of 3D-printed resin groups.

Table 5. Functional groups of FTIR results.

No.	Chemical bonds	Peak wavenumber (cm^{-1})	Vibration characteristics
1	O-H	3425.07	Stretching
2	C-H	2958.20 to 2854.56	Stretching
3	C=O	1728.90	Stretching
4	Ti-O	1609.23	Bending
5	CH_2	1466.79	Bending
6	CH_3	1385.14	Bending
7	C-O-C	1249.39 to 1151.83	Stretching
8	O-CH_3	949.14	Bending
9	C-C	650.61, 471.31	Bending
10	Ba-O	550.55	Bending

Atomic force microscope:

The acquired specimens' topography is displayed in Figure 8. A microscopic examination of atomic force is perfect for quantitatively measuring the surface roughness of specimens in three dimensions. Sa (arithmetic mean height) refers to the crucial surface roughness measurement that gives a broad sense of the sample's elevation and depression of the terrain; it is equivalent to 33.91nm for the control group, 24.71nm for the 0.5 wt.% group, and 18.45nm for the 1 wt.% group. For Sq (root-mean-square height), 0.5 wt.% group has a value of 29.24 nm, while the 1 wt.% specimens display a smoother surface with a value of 22.87 nm. By contrast, the specimens in the control group had the greatest value, measuring 42.03 nm, as the amount of nanoparticle grafting increased, the specimens' roughness decreased, as shown in Table 6.

Table 6. AFM analysis of surface roughness in nanometer.

Group	Sq	Sp	Sv	Sz	Sa	Sku	Ssk
Control	42.03	68.57	124.7	193.3	33.91	2.877	-0.625
0.5 wt.%	29.24	72.20	63.65	135.8	24.71	2.262	-0.04197
1 wt.%	22.87	35.20	62.99	98.25	18.45	2.962	-0.7837

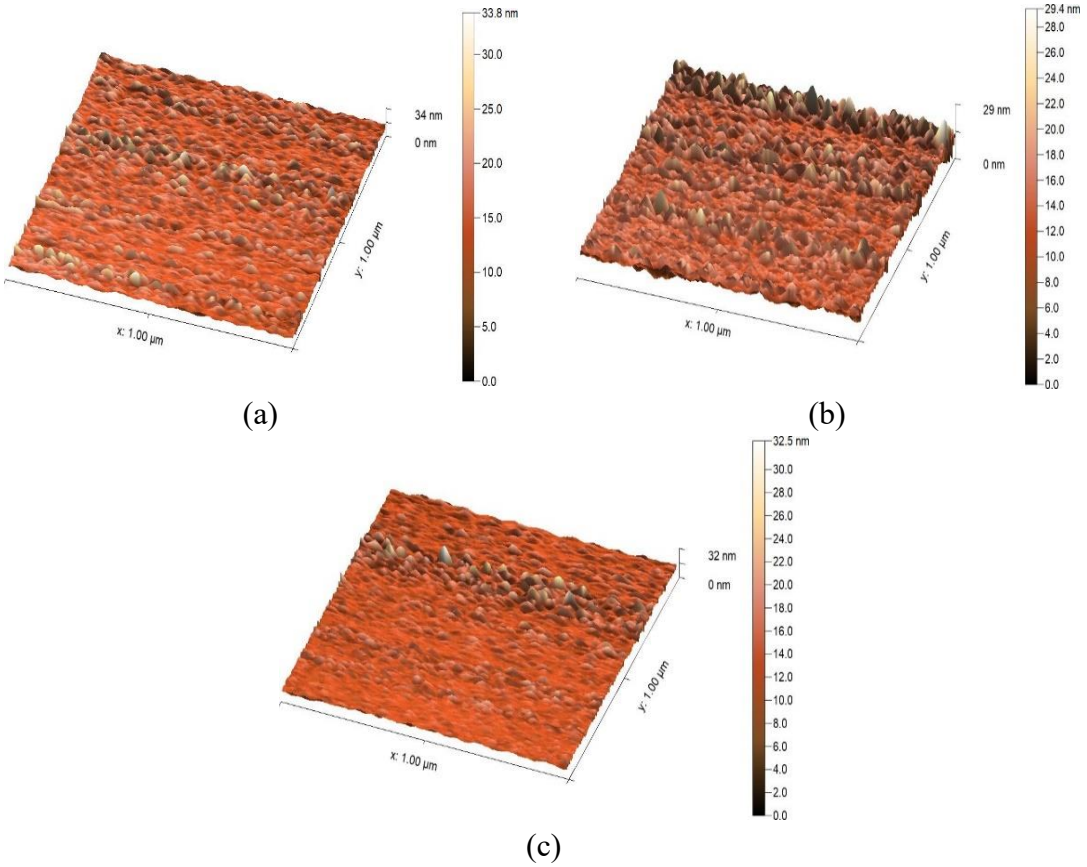

Figure 8. AFM evaluation of the experimental groups (a) Control group specimen (b) 0.5 wt.% group (C) 1 wt.% group.

Discussion:

Broken bits of acrylic dentures can occasionally be swallowed or ingested accidentally. Therefore, having the proper radiopacity for acrylic denture base materials is crucial, because this allows for quicker detection of these pieces before they endanger the patient's life. For the researchers, the creation of radiopaque denture base material is a crucial topic (Mikael et al., 2018).

Since extraoral radiography is frequently utilized as a radiograph in emergency situations, it was used in this study (Mikael et al., 2018). Aluminum has a coefficient of linear absorption that is

comparable to human's structures like enamel, so it is used to normalize the density of exposed films in radiopacity tests (Cook, 1981). International standardization guidelines allow for radiopacity of aluminum up to 2 mm thickness (Powers & Sakaguchi, 2006). Radiopacity increases when radiographic densities decrease. Consequently, in this study by comparing the results with the unmodified group, there was a statistically significant rise in radiopacity (decreased radio densities) as the concentration of barium titanate nanoparticles increased; So, the null hypothesis was rejected. However, 0.5% group was still below the ISO guidelines for radiopacity (accept the radiopacity of 2mm thickness of aluminum). This could be because a material's radiopacity is influenced by its atomic number, with a higher atomic number denoting a more radiopaque material (McCabe & Walls, 2008). In this investigation, $BaTiO_3$ was used as an X-ray contrast material. These outcomes are in line with the discovery of Elshereksi et al., who revealed that the radiopacity of PMMA composites was significantly improved upon by the inclusion of $BaTiO_3$ filler (Elshereksi et al., 2016). Nevertheless, another study that added $BaTiO_3$ NPs to heat-cured PMMA revealed that a proportion of less than 5% did not provide sufficient radiopacity (Ihab & Moudhaffar, 2011).

Denture bases with rough surfaces are more likely to discolor and serve like a breeding ground for microbial adhesion, which results in denture stomatitis. Therefore, a polished denture foundation is required (Gad & Fouda, 2020).

This investigation found that the modified denture base resins exhibit decreased surface roughness (Ra), supported by AFM test results which proved that the roughness of 3D-printing denture foundation decreases with the inclusion of 0.5 weight percent and 1 weight percent $BaTiO_3$NPs. So, the null hypothesis was rejected. Nanofillers can effectively lessen surface roughness and enhance the printed material's resistance to wear (Pagac et al., 2021). We can lower the Ra and reduce surface holes and irregularities by using nanoparticles to fill in the spaces between the polymer matrix (Zidan et al., 2019).

These outcomes are congruent with an earlier study by Mhaibes et al. When compared to the unmodified group, Mhaibes et al. demonstrated that the integration of TiO_2 nanotube into the 3D-printable denture base reduced surface roughness (Mhaibes et al., 2024). Majeed et al. showed the same results when adding yttria stabilized zirconia nanoparticles (YSZNPs) to 3D-printed resin (Majeed et al., 2025).

The current study's results run counter to those of Kumail and Hamad, Gad et al., and Alshaikh et al. When $BaTiO_3$ was added to room-temperature maxillofacial silicone, Kumail and Hamad reported that the surface roughness increased (Kumail & Hamad, 2023). Gad et al. claimed that when SiO_2 was added to 3D-printed resin, the surface roughness raised in comparison to the unmodified group (Gad et al., 2022). According to studies by Alshaikh et al., adding ZrO_2 to 3D-printed resin had no discernible influence on Ra (Alshaikh et al., 2022). The findings imply that Ra might have been more significantly impacted by printing factors and technology, such as layer-by-layer printing and orientation. Ra between layers increased as a result of the specimen surfaces' more compact, stepped edges created by a 90^o printing orientation (Alshaikh et al., 2022).

FTIR analyses were conducted both prior to and following the addition of $BaTiO_3$NPs. There was no chemical reaction that occurred; thus, the addition had no effect on the spectral range. Nanofillers interact with the resin matrix in this instance, and the only contact is described as a physical reaction (Van der Waals bond or hydrogen bond). This interaction appeared as a modification in the intensity of the transmission band of the resin matrix and a little shift in the peak's vibration of bonds that already existed. These results align with the results of research carried out by Khalid et al. (Khalid et al., 2025).

The surface topography and roughness of each 3D-printable resin specimen was examined utilizing AFM both before and after the inclusion of nanoparticles. AFM, sometimes known as scanning probe microscopy, has shown itself to be a very useful technique for examining the surface characteristics of biomaterials at the nanoscale. In contrast to an electron microscope, which provides a 2D image of a specimen, AFM generates an exact 3D profile for the surface (Khadija et al., 2023).

The utilization of just two $BaTiO_3$NPs concentrations and one kind of 3D-printable resin were among the study's limitations. A greater comprehension of the behavior of $BaTiO_3$NPs within the resin matrix would be possible with a higher concentration of NPs. Therefore, in vivo testing is required to clinically validate the information.

It is recommended to evaluate the potential biological hazards and long-term efficacy associated with denture nanocomposites. Investigated how adding $BaTiO_3$ NPs affected the adherence of bacteria and Candida albicans to the materials that served as the basis for 3D-printed dentures. Investigated how $BaTiO_3$ NPs affected the color stability, water absorption, solubility, wettability, shear bonding, and thermal conductivity of 3D-printable denture base substances.

Conclusion:

Inclusion of barium titanate nanoparticles ($BaTiO_3$NPs) in 3D-printable denture bases enhances their radiopacity and reduces surface roughness; the extent of these changes is directly correlated to the concentration of $BaTiO_3$NPs. The influence of $BaTiO_3$NPs on the physical qualities of 3D-printable resin requires more investigation.

Acknowledgments:

The authors are very grateful for the University of Baghdad's ongoing support. We want to express our sincere gratitude to Collage of Dentistry/prosthodontics department for their great help. My sincere appreciation to Professor, Dr. Thekra Ismael Hamad, for her unwavering support and her participation in preparing this work.

Declaration of Competing Interest:

The authors declare that they have no known competing financial interests or personal relationships that could have appeared to influence the work reported in this paper.

Author Contributions:

All authors helped with the research design and execution, the findings analysis, and the drafting of this manuscript: R.N.K. and T.I.H; came up with the concept that was presented.

R.N.K; data gathering and evaluation. The analytical procedure was confirmed by T.I.H. R.N.K; writing-preparation of the first draft. T.I.H; writing-editing and review. T.I.H; supervised and managed the project.

Conflicts of Interests:

There are no conflicts of interest disclosed by the author.

References:

Abd Alrazaq, Y. W., & Khalaf, B. S. (2023). Bond strength of 3d printed acrylic resin with silicone soft liner after ethyl acetate surface treatment (A Review of Literature). *(Humanities, social and applied sciences) Misan Journal of Academic Studies*, *22*(48), 213-225. https://doi.org/10.54633/2333-022-048-016.

ADA. (2000). *Guide to dental materials and devices*. American Dental Association.

Al-Rawi, K. R., & Taha, S. K. (2015). The Effect of nano particles of TiO2-Al2O3 on the Mechanical properties of epoxy Hybrid nanocomposites. *Baghdad Science Journal*, *12*(3), 20. https://doi.org/10.21123/bsj.2015.12.3.597-602.

Al-Rubaie, N. A., & Al-Khafaji, A. M. (2024). Investigation of piranha solution on Color Stability of heat cure acrylic. *(Humanities, social and applied sciences) Misan Journal of Academic Studies*, *23*(51), 17-26 https://doi.org/10.54633/2333-023-051-002.

Al-Sammraaie, M. F., Fatalla, A. A., & Atarchi, Z. R. (2024). Assessment of the correlation between the tensile and diametrical compression strengths of 3D-printed denture base resin reinforced with ZrO2 nanoparticles. *Journal of Baghdad College of Dentistry*, *36*(1), 44-53. https://doi.org/10.26477/jbcd.v36i1.3590.

Al-Dulaijan, Y. A., Alsulaimi, L., Alotaibi, R., Alboainain, A., Akhtar, S., Khan, S. Q., Al-Ghamdi, M., & Gad, M. M. (2023). Effect of printing orientation and postcuring time on the flexural strength of 3D-printed resins. *Journal of Prosthodontics*, *32*, 45-52. https://doi.org/10.1111/jopr.13572

Alghazzawi, T. F. (2016). Advancements in CAD/CAM technology: Options for practical implementation. *Journal of prosthodontic research*, *60*(2), 72-84. https://doi.org/10.1016/j.jpor.2016.01.003

Alshaikh, A. A., Khattar, A., Almindil, I. A., Alsaif, M. H., Akhtar, S., Khan, S. Q., & Gad, M. M. (2022). 3D-printed nanocomposite denture-base resins: effect of ZrO2 nanoparticles on the mechanical and surface properties in vitro. *Nanomaterials*, *12*(14), 2451. https://doi.org/10.3390/nano12142451

Altarazi, A., Jadaan, L., McBain, A. J., Haider, J., Kushnerev, E., Yates, J. M., Alhotan, A., Silikas, N., & Devlin, H. (2024). 3D-printed nanocomposite denture base resin: The effect of incorporating TiO2 nanoparticles on the growth of Candida albicans. *Journal of Prosthodontics*, *33*, 25-34. https://doi.org/10.1111/jopr.13784

Cook, W. D. (1981). An investigation of the radiopacity of composite restorative materials. *Australian Dental Journal*, *26*(2), 105-112. https://doi.org/10.1111/j.1834-7819.1981.tb02443.x

Elshereksi, N., Muchtar, A., & Azhari, C. (2021). Effects of nanobarium titanate on physical and mechanical properties of poly (methyl methacrylate) denture base nanocomposites. *Polymers and Polymer Composites*, *29*(5), 484-496. https://doi.org/10.1177/0967391120926442

Elshereksi, N. W., Mohamed, S. H., Arifin, A., & Ishak, Z. A. (2016). Evaluation of the mechanical and radiopacity properties of poly (methyl methacrylate)/barium titanate-denture base

composites. *Polymers and Polymer Composites*, *24*(5), 365-374. https://doi.org/10.1177/096739111602400507

Gad, M. M., Al-Harbi, F. A., Akhtar, S., & Fouda, S. M. (2022). 3D-printable denture base resin containing SiO2 nanoparticles: An in vitro analysis of mechanical and surface properties. *Journal of Prosthodontics*, *31*(9), 784-790. https://doi.org/10.1111/jopr.13483

Gad, M. M., & Fouda, S. M. (2020). Current perspectives and the future of Candida albicans-associated denture stomatitis treatment. *Dental and medical problems*, *57*(1), 95-102. https://doi.org/10.17219/dmp/112861

Gökay, G. D., Durkan, R., & Oyar, P. (2021). Evaluation of physical properties of polyamide and methacrylate based denture base resins polymerized by different techniques. *Nigerian Journal of Clinical Practice*, *24*(12), 1835-1840. https://journals.lww.com/njcp/fulltext/2021/24120/evaluation_of_physical_properties_of_polyamide_and.12.aspx

Ibrahim, S. W., & Hamad, T. I. (2023). Electrospun nano-barium titanate/polycaprolactone composite coatings on titanium and Ti13Nb13Zr alloy. *Composites and Advanced Materials*, *32*. https://doi.org/10.1177/26349833231203742

Ihab, N., & Moudhaffar, M. (2011). Evaluation the effect of modified nano-fillers addition on some properties of heat cured acrylic denture base material. *Journal of Baghdad College of Dentistry*, *23*(3), 23-29. https://codental.uobaghdad.edu.iq/wp-content/uploads/sites/14/uploads/journal/Ihab%20Final.pdf

ISO. (2013). *ISO 20795-1:2013: Dentistry — Base polymers Part 1: Denture base polymers*. International Organization for Standardization.

Jiang, B., Iocozzia, J., Zhao, L., Zhang, H., Harn, Y.-W., Chen, Y., & Lin, Z. (2019). Barium titanate at the nanoscale: controlled synthesis and dielectric and ferroelectric properties. *Chemical Society Reviews*, *48*(4), 1194-1228. https://doi.org/10.1039/C8CS00583D

Khadija, S. H., Ghassan, A.-H., & Naji, A. R. J. (2023). Title: Enhancing Surface roughness and Wettability of Commercial Pure Titanium Implants with Electrospun PCL/Chitosan/Cinnamon composite. *(Humanities, social and applied sciences) Misan Journal of Academic Studies*, *22*(48), 293-299. https://doi.org/10.54633/2333-022-048-022

Khalid, R. R., Fatalla, A. A., AL-Rawas, M., Johari, Y., Beh, Y. H., & Abdullah, J. Y. (2025). Analysis of thermal conductivity, surface roughness, and hardness of carbon nanotube-reinforced three-dimensional printed acrylic resin. *Baghdad Science Journal*, *22*(5), 1609-1620. https://doi.org/10.21123/bsj.2024.11832

Kumail, A. F., & Hamad, T. I. (2023). Impact of Shore A hardness and Surface roughness of Room Tem-perature Maxillofacial Silicone after the addition of Nano Barium Titanate. *Bionatura*, *8*(3), 1-7. http://dx.doi.org/10.21931/RB/CSS/2023.08.03.88

Majeed, H. F., Hamad, T. I., & Al-Salihi, Z. (2025). Yttria stabilized zirconia: innovative approach for improving the performance of additively manufactured denture resins. *Journal of Baghdad College of Dentistry*, *37*(2), 27-36. https://doi.org/10.26477/jbcd.v37i2.3965

McCabe, J. F., & Walls, A. W. G. (2008). *Applied Dental Materials*. Wiley-Blackwell.

Mhaibes, A. H., Safi, I. N., & Haider, J. (2024). The influence of the addition of titanium oxide nanotubes on the properties of 3D printed denture base materials. *Journal of Esthetic and Restorative Dentistry*, *36*(11), 1574-1590. https://doi.org/10.1111/jerd.13299

Mikael, J., Al-Samaraie, S., & Ikram, F. (2018). Evaluation of Some Properties of Acrylic Resin Denture Base Reinforced with Calcium Carbonate Nano-Particles. *Erbil Dental Journal*, *1*(1), 41-47. https://doi.org/10.15218/edj.2018.06

Noori, Z. S., Al-Khafaji, A. M., & Dabaghi, F. (2023). Effect of tea tree oil on candida adherence and surface roughness of heat cure acrylic resin. *Journal of Baghdad College of Dentistry*, *35*(4), 46-54. https://doi.org/10.26477/jbcd.v35i4.3513

Pagac, M., Hajnys, J., Ma, Q.-P., Jancar, L., Jansa, J., Stefek, P., & Mesicek, J. (2021). A review of vat photopolymerization technology: materials, applications, challenges, and future trends of 3D printing. *Polymers*, *13*(4), 598. https://doi.org/10.3390/polym13040598

Powers, J. M., & Sakaguchi, R. L. (2006). *Craig's restorative dental materials*. Mosby, Missouri. https://cir.nii.ac.jp/crid/1570009751456219264

Tian, Y., Chen, C., Xu, X., Wang, J., Hou, X., Li, K., Lu, X., Shi, H., Lee, E.-S., & Jiang, H. B. (2021). A review of 3D printing in dentistry: Technologies, affecting factors, and applications. *Scanning*, *2021*, 9950131. https://doi.org/10.1155/2021/9950131

Unkovskiy, A., Schmidt, F., Beuer, F., Li, P., Spintzyk, S., & Kraemer Fernandez, P. (2021). Stereolithography vs. direct light processing for rapid manufacturing of complete denture bases: an in vitro accuracy analysis. *Journal of clinical medicine*, *10*(5), 1070. https://doi.org/10.3390/jcm10051070

Zidan, S., Silikas, N., Alhotan, A., Haider, J., & Yates, J. (2019). Investigating the mechanical properties of ZrO2-impregnated PMMA nanocomposite for denture-based applications. *Materials*, *12*(8), 1344. https://doi.org/10.3390/ma12081344

تأثير جزيئات الباريوم تيتانيت النانوية على القدرة الاشعاعية وخشونة السطح الأكريليك المطبوع ثلاثي الأبعاد

رند نصير كاظم، ذكرى إسماعيل حمد

قسم التعويضات السنية، كلية طب الاسنان، جامعة بغداد، بغداد، العراق

المستخلص:

أصبح من الممكن تصنيع قاعدة طقم الأسنان ثلاثي الأبعاد بفضل ظهور تقنية التصنيع بالإضافة. يهدف هذا البحث الى فحص تأثيرات إضافة جزيئات الباريوم تيتاينت النانوية بنسب وزنية مختلفة على القدرة الشعاعية وخشونة السطح للراتينج أكريليك قاعدة طقم الاسنان المطوع ثلاثي الابعاد. تم تقسيم العينات الى ثلاث مجموعات: مجموعة المراقبة، 0.5%،1 % من جزيئات الباريوم تيتاينت النانوية. كل عينة خضعت لاختبار خشونة السطح بواسطة جهاز قياس الارتفاع وجهاز مجهر القوة الذرية، تم قياس القدرة الشعاعية باستخدام جهاز الكثافة الضوئية. مقارنة مع مجموعة المراقبة، إضافة جزئيات الباريوم تيتانيت النانوية الى راتينج المطبوع ثلاثي الابعاد حسنت القدرة الشعاعية لمجموعة الاضافة. خشونة السطح تناقصت بعد إضافة جزيئات الباريوم تيتانيت النانوية مقارنة مع مجموعة المراقبة.

الكلمات المفتاحية: مجهر القوة الذرية، جزيئيات الباريوم تيتانيت النانوية، القدرة الشعاعية، خشونة السطح، قاعدة طقم ثلاثية الابعاد.